Development of *in situ* high resolution NMR: Proof-of-principle for a new (spinning) cylindrical mini-pellet approach applied to a Lithium ion battery

Irshad Mohammad [a,**,1], Musa Ali Cambaz [b], Ago Samoson [a], Maximilian Fichtner [b,c], Raiker Witter [a,b,c,d,*]

[a] *Laboratory of Spin Design, Institute of Cybernetics, Tallinn University of Technology, Ehitajate Tee 5, 19086, Tallinn, Estonia*
[b] *Helmholtz-Institute Ulm for Electrochemical Energy Storage (HIU), Helmholtzstr. 11, 89081, Ulm, Germany*
[c] *Institute of Nanotechnology, Karlsruhe Institute of Technology (KIT), POB 3640, 76021, Karlsruhe, Germany*
[d] *Institute of Quantum Optics, University Ulm, Albert-Einstein-Allee 11, 89081, Ulm, Germany*

Keywords:
Lithium-ion battery
^{7}Li MAS NMR
Li metal
VO_2F intercalation cathode
Cylindrical cell design

A B S T R A C T

Solid-state nuclear magnetic resonance (ssNMR) spectroscopy is a powerful technique for characterizing the local structure and dynamics of battery and other materials. It has been widely used to investigate bulk electrode compounds, electrolytes, and interfaces. Beside common *ex situ* investigations, *in situ* and *operando* techniques have gained considerable importance for understanding the reaction mechanisms and cell degradation of electrochemical cells.

Herein, we present the recent development of *in situ* magic angle spinning (MAS) NMR methodologies to study batteries with high spectral resolution, setting into context possible advances on this topic. A mini cylindrical cell type insert for 4 mm MAS rotors is introduced here, being demonstrated on a Li/VO_2F electrochemical system, allowing the acquisition of high-resolution ^{7}Li MAS NMR spectra, spinning the electrochemical cell up to 15 kHz.

1. Introduction

Present day electrochemical standards are set by the lithium-ion battery (LIBs) technology regarding energy density, cycling stability, high cell voltage and various applications. It also holds perspectives for further performance boost by the introduction of advanced electrodes, e. g. silicon anode and fluorinated cathodes [1,2]. Cyclic performance of LIBs strongly depends upon the EEI (electrode-electrolyte interface), like SEI (solid-electrolyte interface) and CEI (cathode electrolyte interface), and electrode materials. During charge/discharge processes, electrodes may go through structural changes, electrolyte may decompose at the SEI/CEI, dendrites may form, and electrodes may increase inactive content or undergo adverse microscopic changes. As to the present day, there are number of analytical techniques commonly available to study composition, reaction mechanism and degradation of electrode materials during functional operation of the electrochemical structures such as X-ray diffraction, electron microscopy (e.g. SEM and TEM), X-ray photoelectron spectroscopy (XPS), X-ray absorption spectroscopy (XAS), nuclear magnetic resonance (NMR) and electron paramagnetic resonance spectroscopy (EPR) [3–10]. Above all, NMR spectroscopy is an important tool for understanding the fundamental processes that occur during charge and discharge process of batteries, especially when none-crystalline effects play a fundamental role within the bulk material [11,12].

As to date, the $^{6/7}$Li NMR of entire battery assemblies enables the detection and quantification of different lithium-containing species, such as lithium ions in the electrolyte, electrode materials, dendrite/metal-cluster related sites, and species formed due to electrode-electrolyte interactions [13–16]. *In situ* and *operando* NMR techniques are a valuable tool for studying battery chemistry, providing real-time information about the inner workings of batteries and helping to optimize their performance and safety.

A number of attempts have been made to improve *in situ* capabilities that have better reliability, sensitivity, and longevity, where the first *in situ* NMR analysis was presented by Gerald et al. [17]. In their work, a compression coin cell battery imager used to perform NMR experiments

* Corresponding author. Laboratory of Spin Design, Institute of Cybernetics, Tallinn University of Technology, Ehitajate tee 5, 19086, Tallinn, Estonia.
** Corresponding author.
E-mail address: raiker.witter@ttu.ee (R. Witter).
[1] Present Address **Irshad Mohammad -** Battery Technologies, Center for Low-emission Transport AIT Austrian Institute of Technology GmbH Giefinggasse 4, 1210 Vienna (Austria).

through the entire cycling process, enabling to obtain spectra from various fractions of lithium ions in their different local environments. In the cell assembly, a flat metal conductor of circular shape was used which serves as an NMR detector as well as current collector. Two spectral regions were observed which can originate from multiple nuclear interactions, like the unpaired electron spin conduction band contribution, chemical shift, paramagnetic shifts, quadrupolar and dipolar couplings [13], each being also dependent on local coordinate orientation. In the first region, total shifts around 12–17 ppm correspond to fully lithiated graphite, whereas the second peak region at higher chemical shift values (260–290 ppm) is related to metallic contributions without indication of possible dendrite formation. The spectral region between 0 and 10 ppm contains the information about SEI components (e.g. LiF, $LiCO_3$, LiO_2, LiR, and LiOR) [18,19], which were not extracted due to the lack of resolution. A further advancement was introduced by Letellier et al. and Bellcore et al. who introduced a plastic bag batteries configuration and implemented it into a static *in situ* NMR setup, successfully applied for the identification of electrochemical products in hard carbon and graphite [20–22]. ^{7}Li NMR spectra obtained reveal fully intercalated graphite Li_xC_6 (x = 1.078) at 40 ppm with quadrupolar satellites, vanishing during lithium extraction. An intense and broad peak at 2 ppm was determined to correspond to mainly $LiPF_6$. Here again, SEI and other species were not resolved.

Most of the *in situ* NMR studies are performed on batteries utilising carbon electrodes, some of the studies use layered oxide cathodes [23–25]. Key et al. reported studies on silicon anodes for LIBs using Bell core based cell configuration [7], where *in* and *ex situ* NMR was carried out. It was demonstrated that *in situ* experiments monitor the molecular changes that cannot be readily seen by *ex situ* methods. Such *in situ* investigations reveal the formation of metastable crystalline $Li_{15}Si_4$, which was not detectable by *ex situ* due to the fact that the over-lithiated $Li_{15}Si_4$ phase easily reacts with electrolyte after cell disassembling.

Pushing the technology beyond discussed flat-cell configurations, Fabrizia Poli et al. introduced a new cylindrical cell design for *in situ* NMR studies of LIBs [26]. This configuration had been intended being a more convenient cell assembly with simplified operation, whilst providing a larger coil filling factor for signal enhancement. It is also suitable for usage of powdered materials. The applicability of this cell configuration was demonstrated by performing *in situ* ^{31}P NMR of a Cu_3P/Li battery. Although the study demonstrated mechanism of lithium insertion and extraction of Cu_3P, it does not reveal sufficient information on SEI components. The cell design increases the sensitivity significantly, but the resolution remains limited by orientational/anisotropy effects, pertinent to static samples. First high resolution *in situ* MAS NMR investigations of LIBs were performed by Freytag et al. using jelly roll cell design [27]. Unlike flat or coin cells, a jelly roll type battery has a rotational symmetry and uses minimum metallic components (active materials casted onto a cellulosic substrate instead of copper and aluminium; and titanium wires used as current collectors) rendering it very suitable for spinning at high rates at the magic angle within a strong magnetic field. The state of the art was applied on a LIB system comprising of $LiCoO_2$ cathode and graphite anode. *In situ* MAS NMR measurements were successfully performed at spinning speeds up to 10 kHz without destroying the cell and providing qualitatively new level of data. An overview of previous *in situ/operando* NMR studies for batteries are given in Table 1.

Here, we report a high resolution MAS NMR approach of cylindrical mini-pellet (entire) battery at a spinning rate up to 15 kHz [34] for a proof-of-concept *in situ* ^{7}Li MAS NMR study of a Li/$LiPF_6$/VO_2F cell. We first address some practical challenges occurred during employing high resolution NMR, then discuss details about the cylindrical cell design used for performing magic angle spinning, finally provide NMR spectral results and shortly discuss findings.

Table 1
Overview of previous NMR studies of LIBs.

Authors	Cell type	Analysing sytem	Outcomes
Gerald et al. [17]	Compression coin cell	Li||Carbon	Metallic lithium and lithiated graphite identified
Letellier et al. [20]	Plastic bag cell	Li||Graphite	Electrolyte and Intercalation of graphite
Key et al. [7]	Plastic bag cell	Li||Si	Identification of meta stable crystalline $Li_{15}Si_4$ phase
Shimoda et al. [24]	Plastic bag cell	Li||$LiCoO_2$	Quantitative information on lithium environments in cathode, anode, and electrolyte simultaneously
Fabrizia Poli et al. [26]	Cylindrical cell	Li||Cu_3P	Mechanism of lithium insertion and extraction of Cu_3P
Freytag et al. [27]	Jelly roll cell	Graphite|| $LiCoO_2$	The state of charge, metallic lithium plating and SEI formation
Gunnarsdóttir et al. [12]	Capsule cell	Cu||$LiFePO_4$	Dead lithium and SEI formation was quantified
Feng et al. [28]	Bag cell	Li||Ni_5P_4	Lithiation and delithiation mechanisms for Ni_5P_4 electrode
Sorte et al. [29]	Pouch cell	Graphite|| $LiFePO_4$ or $LiCoO_2$	This study focused on higher detection sensitivity and sample filling factor
Kayser et al. [4]	Plastic based Swagelokcell	Li||Graphite	Revealing the formation and evolution of mossy and dendritic Li microstructure on long cycling
Pecher et al. [30]	Plastic bag cell	Li||$LiFePO_4$ and Na|| $Na_3V_2(PO_4)_2F_3$	formation of intermediate phases and electrolyte decomposition during electrochemical cycling of Li- and Na-ion batteries
Walder et al. [31]	Coin cell	β-LiAl||Li_xMnO_2	NMR measurements of an unmodified commercial coin cell with metal casings, real time changes lithium diffusion in the electrodes
Märker et al. [32]	Capsule cell	Graphite|| NMC811	Operando NMR study of commercial type lithium ion batteries
Gauthier et al. [33]	Cylindrical cell	Li||O_2	Mossy Li/Li dendrites and other irreversible parasitic lithium compounds

2. Electrode preparation

The crystalline host material VO_2F was prepared by previously reported procedure [35]. The compound was synthesized by high energy milling of stoichiometric amounts of V_2O_5 (99.6 %, Sigma Aldrich) and VOF_3 (99 %, Sigma Aldrich) for 24 h under an inert atmosphere. Milling was performed using vial (80 ml) and balls (10 mm diameter) made of ZrO_2. After ball milling, powder was taken out from the jar and stored in the glove box. The VO_2F composite was prepared by mixing as-milled VO_2F (75 wt %), carbon black (15 wt %), and PVDF (10 wt %) using mortar and pestle inside Ar-filled glove box. The pellets were prepared by uniaxial pressing of VO_2F composite by home machined pressing tool. The diameter and thickness of the pellet were determined to be approximately 2.8 and 1.0 mm, respectively. Commercially available

graphite rod was obtained from Polytron Kunststofftechnik GmbH. The Li metal foil (Sigma Aldrich) with thickness of 0.75 mm was cut into a disc with diameter of 2.8 mm (mass of 2.46 mg), which was used as negative electrode. 1 M $LiPF_6$ solution in EC:DMC (1:1) were used as anode and electrolyte, and Whatman GF/D glass microfiber sheets (675 μm thickness) were used as separator. The discharging of the LIB cell was performed by a Keysight N6705B (DC power analyser) battery tester.

3. Cell assembly

A sketch of the discharging cylindrical battery in opened 4 mm rotor sleeve is shown in Fig. 1. The encapsulated cell consists of a Vespel polymer cylindrical insert, and two caps made of graphite-polymer material, also acting as current collectors. The inner and outer diameter of the insert was 2.8, and 3.0 mm, respectively, with a length of 5 mm. Both, insert with caps, have same outer diameter fitting to the inner rotor dimension (3 mm), and keeping the rotor balanced during spinning. The length of the whole battery was prepared being equal to the length of the insert with caps for ensuring mechanical stability during spinning and electrical contact during discharging, see Fig. S1a. Assembling the battery was performed under argon atmosphere in a glove-box system (Fig. 1). First, the cathode pellet was placed in the insert; next one micro fibre separator soaked with LiF_6 electrolyte was put on top; then a thin pellet of lithium foil was added, and in the last step, graphite caps were used to close the insert from both ends. The cathode pellet was pressed by a homemade tool-set given in Fig. S1b. Also, a home-made Swagelok type battery holder was manufactured to discharge the tiny LIB battery present in Fig. S1c.

4. MAS NMR of mini pellet based cell

A detailed schematics of the MAS NMR rotor set-up is shown in Fig. 2. Before closing the rotor, two spacers were placed inside from top and bottom ends, in order to keep the insert containing the cell stable whilst spinning the rotor (Fig. 2). The spacers were made of cellulose fibre and were used to keep the rotor light weight and balanced. To perform MAS NMR experiments, the rotor containing battery was transferred into turbine housing, containing a solenoid coil (20 mm in length) of a home build MAS NMR probe.

^{7}Li MAS NMR measurements were performed on the Li/VO_2F cell at pristine and discharge state. Various spinning speeds were used to acquire the spectra. All NMR experiments were carried out at on a 400 MHz Bruker Advance spectrometer. Spectra were recorded in open circuit mode using a 90° pulse length of 2 μs collecting 512 scans. For spectral referencing, aqueous solution of LiCl was used.

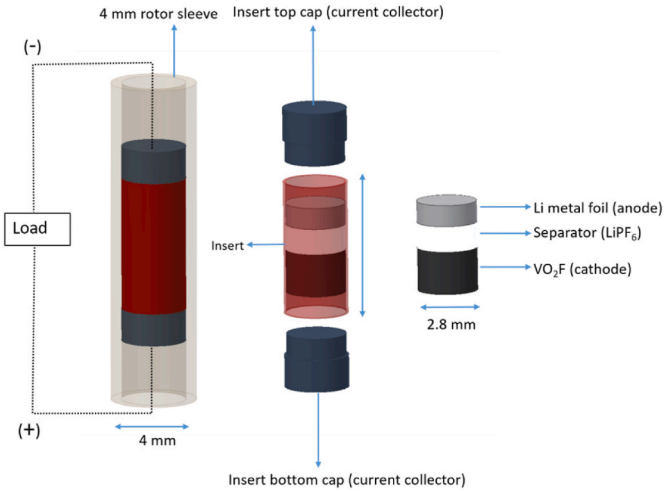

Fig. 1. Schematic of sketch of new cell design with rotor sleeve.

5. Result and discussion

After assembling the battery pellet into the insert as described in Fig. 1, the open circuit voltage (OCV) of Li/VO_2F cell was measured being about 3.8 V, indicating a good connection between battery components. Then, the insert containing battery sample was transferred into a rotor for NMR measurements, Fig. 3 (top layer) shows the limited spectral resolution of the static ^{7}Li NMR spectrum of the battery in as assembled state. Two peaks were observed with chemical shift of 263 ppm, and a broad peak around 0 ppm, consistent with previous reports [20]. The metallic peak (attributed to the Knight Shift originating from unpaired electron contributions of the conduction band electrons) shows two major line contributions, corresponding to the rf-field penetration depths vs. geometric susceptibility effects [13]: one line corresponds to the pristine Li bulk metal foil; the other to Li mossy-structures deposited on the metal surface [33,36]. The tip of the graphite cap has sharp edges scratching and binding some lithium foil during cell assembly. The bottom trace in Fig. 3 shows a MAS NMR spectrum of the battery at slow spinning rate of 2.5 kHz. Unlike in the static spectrum, here we observed a resolution enhancement of the peak around 0 ppm. Remaining anisotropic contributions are observable in the spinning side bands left and right to the central isotropic line.

Notably, the peak of the Li foil has completely vanished with spinning in the magnetic field. The rotated metal foil in the magnet creates eddy currents which generate heat depending upon the dimensions of metal foil, rotation speed, nature of metal, and magnetic field. Since we are using a thin Li metal foil (2.8 mm diameter) with mossy metal, the generation of heat due to eddy current was reduced preventing sample destruction. Aapart from eddy current, the spinning lithium metal foil generates local susceptibility and electric field distributions causing a chemical shift dispersion of lithium foil rendering the signal between 200 and 400 ppm region unobservable [37]. Same spectrum profile was also obtained at spinning speed of 1.25 kHz, depicted in Fig. S2.

The broad overlapping peak feature (half width around 700 Hz) in the 4 to 12 ppm region can be attributed to combination of Li ions in free electrolyte ($LiPF_6$), Li ions of electrolyte soaked separator, the SEI, electrolyte adsorbed within the cathode, the CEI and from the lithiated cathode itself [21,38,39]. Since Li ions in free electrolyte undergo rapid molecular tumbling, anisotropic interactions averaging out which leads to sharper spectral features at around 0 ppm. The Li ions shift dispersion and broadening also reflect the local environment with a specific magnetic susceptibility distribution which, for instance in case of $LiPF_6$, are electrolyte in soaked separator, in the cathode material or at the surface of the metal anode. The reductive dissolution of electrolyte on the electrode surface leads to formation of SEI/CEI layers which protects electrolyte from further decomposition. The spectral contribution of SEI formation has been reported to range from 10 to 10 ppm [40].

To discharge the cell for further analysis, we took the rotor containing the LIB mini-pellet out of the NMR probe, transferred to the glove-box, opened the insert sleeve from both ends to connect it to wires to the battery tester (Fig. 1) for unloading to a partially discharged state of 1 V.

Fig. 4a shows the discharge curve of the mini-pellet battery at the rate of C/20. The electrochemical behaviour of VO_2F cathode looks same as the reported in the literature [35]. Static and MAS NMR spectra of the partially discharged cell is shown in Fig. 4 b to d. In the static spectrum, two signals were observed with a shift at around 260 ppm related to Li metal. The first signal at 250 ppm is related to pristine Li metal, whereas second signal at 267 ppm assigned to Li mossy-structures deposited on the bulk metal surface [33,36]. In the spectrum, two broad peaks overlapped to each other were observed in the range from 140 to 140 ppm, assigned to Li_xVO_2F ($x \leq 1$) and Li_xVO_2F ($x \leq 2$)[41]. The line width was found being around 15 kHz, much larger than for the pristine (100 Hz) state. In pure VO_2F, the vanadium oxidation state is +5, which changes to +4 or +3 after lithiation, creating local paramagnetism causing line broadening. Furthermore, the appearance of the two big Li

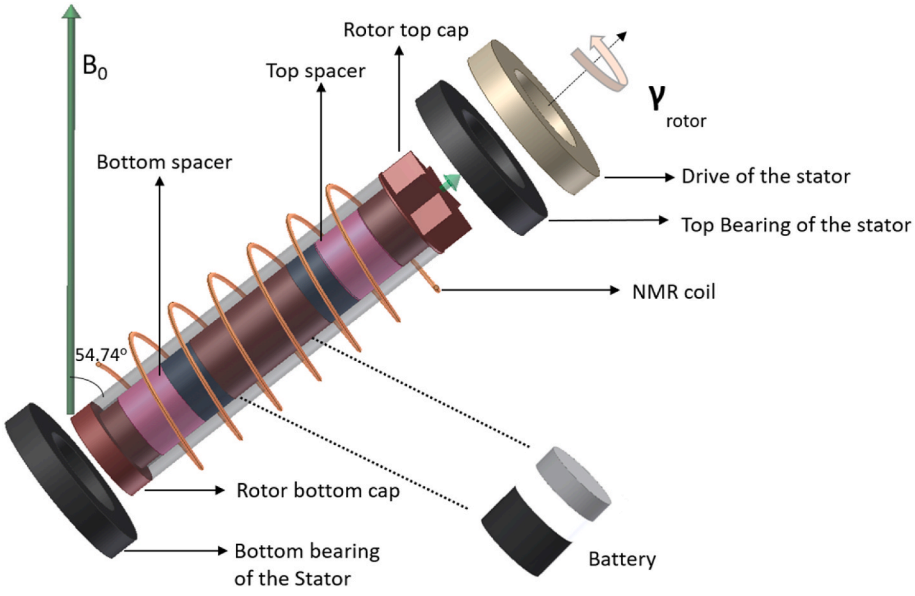

Fig. 2. Schematic of MAS NMR setup: the assembled $VO_2F/LiPF_6$/Li LIB pellet was placed in the rotor with graphite caps as current collectors and spacers for mechanically stabilizing the insert assembly.

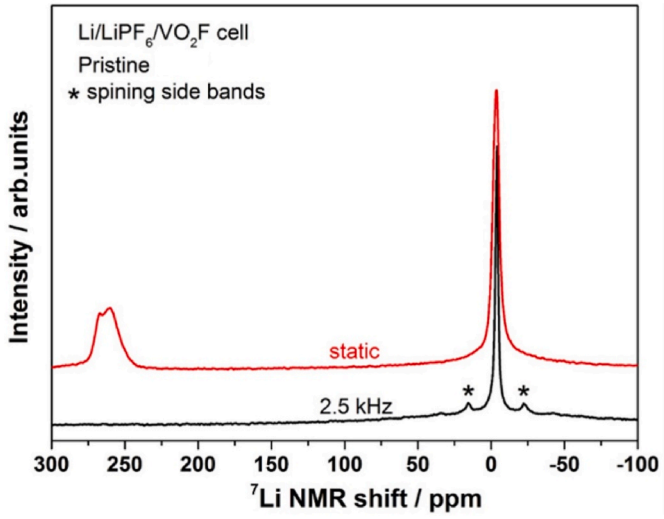

Fig. 3. (a) Static and MAS ^{7}Li NMR spectra of a $VO_2F/LiPF_6$/Li LIB mini-pellet in pristine state.

metal peaks at a partially discharged state indicates that anode was used in excess. The broad line contributions in the range of 140 to 140 ppm results from an overlap of peaks attributed to electrolyte in the separator, soaked electrolyte (cathode), SEI, adsorbed Li ions on electrode and intercalated Li ions (cathode).

Starting to spin the cell at 2.5 kHz MAS (see Fig. 4c), the peak region around 110 to 110 ppm could be deconvoluted into three components: first two are related to Li_xVO_2F ($x \leq 1$ & $x \leq 2$) including cathode electrolyte interface, and the third being significantly sharper (diamagnetic) at 3.6 ppm corresponding to SEI + $LiPF_6$[27]. Associated spinning side bands are indicated in the spectrum with stars. Remaining mossy Li-metal contributions (incl. side-bands) were observed at around 263 ppm. The broad overlapping signals (around 0 ppm) were assigned to combination of resonances from the SEI, adsorbed Li ions on electrode surface and Li ions intercalated into the host VO_2F [41]. The line width significantly reduced to 300 Hz being considerably less than in the static case: resolution enhancement is about 5.

Since we applied 50 % higher MAS rates on a spinning battery (15 kHz) than previously reported (10 kHz) [27], centrifugal force can be suspected to decompose the pellet assembly. We repeated the experiment for several pellets and confirmed mechanical and thermal stability. The morphological stability of cell assembly and pellet after MAS (15 kHz) can be deduced from Fig. S3 a and b. As we can be observed from the figure, the pellet did not break even after spinning the assembly for several hours, the Li-foil is in place (Li melting point is at 180.5 °C). However, it is worth to mention that the pellet assembly approach may be limited due usage of critical metallic lithium foil thickness and reduced porosity, which can heat up the battery due to generated eddy currents. Another drawback could be the limited amount of in depth active material reaction due the pellet based assembly. The MAS spectrum of a 15 kHz rotated battery is represented in Fig. 4d. The resolution of the obtained spectra was considerably improved. After curve fitting, peaks corresponding to Li_xVO_2F ($x \leq 1$) and Li_xVO_2F ($x \leq 2$) could be separated and their resonances assigned to 4,2, and 9.3 ppm [41]. Additionally, a resonance at 3,4 ppm was observed which can be attributed to SEI + $LiPF_6$[27]. Again, the new metallic feature with the shift of 261 ppm can be attributed to lithium in a porous or nano-structure formation of the foil.

6. Conclusions

A cylindrical mini pellet design has been introduced and proof-of-principle *in situ* MAS NMR experiments on a related complete cell assembly accomplished. After transferring the cell pellet into the rotor, first static and then MAS ^{7}Li NMR spectra of the pristine (charged) Li/$LiPF_6$/VO_2F system were acquired to observe signals from every part of the battery. Then, after partial discharge to 1 V, again static and MAS ^{7}Li NMR were recorded in the common *in situ* manner, i.e. using the same insert with pellet. The spectral resolution considerably enhanced to gain more information of SEI/$LiPF_6$ and differentiate between Li_xVO_2F ($x \leq 1$) and Li_xVO_2F ($x \leq 2$) contributions. Further, a new Li metal peak at 261 ppm of partially discharged LIB cell was detected, possibly attributed to porous nano-cluster mossy-structure formations.

It has to be taken care about metallic lithium dimensions and morphology because it can cause serious heating of the sample through generated eddy current. Pellet based electrodes have reactive area confined only to base of the cylinder. Advantage of this design compared

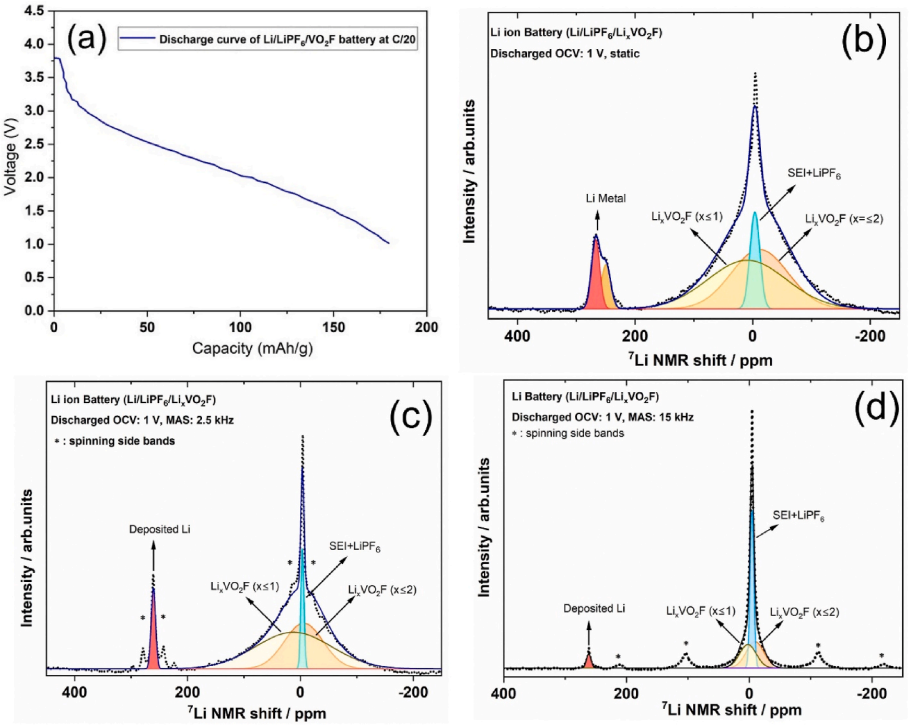

Fig. 4. (a) The discharge curve of the mini-pellet based cell is shown. ^{7}Li NMR spectra of the partially discharged (1 V) state are depicted in: (b) static, (c) spinning at 2.5 kHz, and (d) spinning at 15 kHz.

to jelly roll design is that we can perform spatial resolved MAS NMR using slice selection along spinning axis.

This new mini-pellet design enabled a straightforward cell preparation and high-spectral resolution NMR investigations. The design is well suitable for *in situ* MAS NMR investigations on whole battery assembles at various stage of charge. Notably, this design permits stable spinning of battery pellets up to 15 kHz, improving practical resolution by a factor up to 50, enabling an advanced signal deconvolution and site assignment. This mini-pellet setup opens up improved capabilities of conducting critical informative with the aid of high-resolution solid-state MAS NMR and opens a wide range of opportunities for various aspects and types of battery chemistries, in order to understand and improve electrochemical cell performance.

Supporting information

Picture of battery insert, home machined tools for pellet press, homemade battery holder, NMR spectrum of battery at spinning speed of 1.25 kHz. Also, a post-mortem photograph of the cell assembly and pellet after MAS is provided.

Author contributions

Irshad Mohammad and Raiker Wittter designed and performed the research and analyzed data. Musa Ali Cambaz prepared the VO2F cathode. Irshad Mohammad designed, constructed, and tested the MAS 15-kHz system (probe, rotation, and rotor tools) under supervision of Raiker Witter. Irshad Mohammad wrote the manuscript. All authors read and approve the final manuscript.

Funding

Many thanks to European Social Fund, Estonia Science Foundation (ESF), Tallinn University of Technology (TalTEch) for funding project MTT68, PUT126, PUT1534, PRG1832, STP57 financial/infrastructural support from the NMRI lab, Karlsruhe Institute of Technology (KIT), program Nano-Micro and Karlsruhe Nano Micro Facility (KNMF). This work was further supported by CELEST (Center for Electrochemical Energy Storage Ulm-Karlsruhe) and by the German Research Foundation (DFG) under Project ID 390874152 (POLiS Cluster of Excellence).

Declaration of competing interest

We have no conflicts of interest to disclose.
All authors declare that they have no conflicts of interest.

Data availability

No data was used for the research described in the article.

Acknowledgments

We thank Meelis Rohtmäe for machining the pressing tools, battery inserts and their caps.

References

[1] A. Franco Gonzalez, N.-H. Yang, R.-S. Liu, Silicon anode design for lithium-ion batteries: progress and perspectives, J. Phys. Chem. C 121 (50) (2017) 27775–27787, https://doi.org/10.1021/acs.jpcc.7b07793.
[2] K. Lemoine, A. Hémon-Ribaud, M. Leblanc, J. Lhoste, J.-M. Tarascon, V. Maisonneuve, Fluorinated materials as positive electrodes for Li- and Na-ion batteries, Chem. Rev. 122 (18) (2022) 14405–14439, https://doi.org/10.1021/acs.chemrev.2c00247.
[3] M. Balasubramanian, X. Sun, X.Q. Yang, J. McBreen, In situ X-ray diffraction and X-ray absorption studies of high-rate lithium-ion batteries, J. Power Sources 92 (1) (2001) 1–8, https://doi.org/10.1016/S0378-7753(00)00493-6.
[4] S.A. Kayser, A. Mester, A. Mertens, P. Jakes, R.-A. Eichel, J. Granwehr, Long-run in operando NMR to investigate the evolution and degradation of battery cells, Phys.

Chem. Chem. Phys. 20 (20) (2018) 13765–13776, https://doi.org/10.1039/C8CP01067F.
[5] W.-S. Yoon, C.P. Grey, M. Balasubramanian, X.-Q. Yang, J. McBreen, In situ X-ray absorption spectroscopic study on LiNi0.5Mn0.5O2 cathode material during electrochemical cycling, Chem. Mater. 15 (16) (2003) 3161–3169, https://doi.org/10.1021/cm030220m.
[6] M. Carewska, S. Scaccia, F. Croce, S. Arumugam, Y. Wang, S. Greenbaum, Electrical conductivity and 6,7Li NMR studies of Li1 + yCoO2, Solid State Ionics 93 (3) (1997) 227–237, https://doi.org/10.1016/S0167-2738(96)00545-0.
[7] B. Key, R. Bhattacharyya, M. Morcrette, V. Seznéc, J.-M. Tarascon, C.P. Grey, Real-time NMR investigations of structural changes in silicon electrodes for lithium-ion batteries, J. Am. Chem. Soc. 131 (26) (2009) 9239–9249, https://doi.org/10.1021/ja8086278.
[8] A.M. Andersson, D.P. Abraham, R. Haasch, S. MacLaren, J. Liu, K. Amine, Surface characterization of electrodes from high power lithium-ion batteries, J. Electrochem. Soc. 149 (10) (2002) A1358, https://doi.org/10.1149/1.1505636.
[9] S.V. Kalinin, N. Balke, Local electrochemical functionality in energy storage materials and devices by scanning probe microscopies: status and perspectives, Adv. Mater. 22 (35) (2010) E193–E209, https://doi.org/10.1002/adma.201001190.
[10] Y. Xiang, X. Li, Y. Cheng, X. Sun, Y. Yang, Advanced characterization techniques for solid state lithium battery research, Mater. Today 36 (2020) 139–157, https://doi.org/10.1016/j.mattod.2020.01.018.
[11] N.M. Trease, L. Zhou, H.J. Chang, B.Y. Zhu, C.P. Grey, In situ NMR of lithium ion batteries: bulk susceptibility effects and practical considerations, Solid State Nucl. Magn. Reson. 42 (2012) 62–70, https://doi.org/10.1016/j.ssnmr.2012.01.004.
[12] A.B. Gunnarsdóttir, C.V. Amanchukwu, S. Menkin, C.P. Grey, Noninvasive in situ NMR study of “dead lithium” formation and lithium corrosion in full-cell lithium metal batteries, J. Am. Chem. Soc. 142 (49) (2020) 20814–20827, https://doi.org/10.1021/jacs.0c10258.
[13] O. Pecher, J. Carretero-González, K.J. Griffith, C.P. Grey, Materials’ methods: NMR in battery research, Chem. Mater. 29 (1) (2017) 213–242, https://doi.org/10.1021/acs.chemmater.6b03183.
[14] C.P. Grey, N. Dupré, NMR studies of cathode materials for lithium-ion rechargeable batteries, Chem. Rev. 104 (10) (2004) 4493–4512, https://doi.org/10.1021/cr020734p.
[15] J.Z. Hu, N.R. Jaegers, M.Y. Hu, K.T. Mueller, In situ and ex situ NMR for battery research, J. Phys. Condens. Matter 30 (46) (2018), 463001, https://doi.org/10.1088/1361-648X/aae5b8.
[16] A.L. Michan, G.T.M. Nguyen, O. Fichet, F. Vidal, C. Vancaeyzeele, C.A. Michal, Nuclear magnetic resonance (NMR) characterization of a polymerized ionic liquid electrolyte material, MRS Online Proc. Libr. 1440 (1) (2012) 31–36, https://doi.org/10.1557/opl.2012.1280.
[17] R.E. G II, J. Sanchez, C.S. Johnson, R.J. Klingler, J.W. Rathke, In situ nuclear magnetic resonance investigations of lithium ions in carbon electrode materials using a novel detector, J. Phys. Condens. Matter 13 (36) (2001) 8269, https://doi.org/10.1088/0953-8984/13/36/304.
[18] E. Peled, The electrochemical behavior of alkali and alkaline earth metals in nonaqueous battery systems—the solid electrolyte interphase model, J. Electrochem. Soc. 126 (12) (1979) 2047, https://doi.org/10.1149/1.2128859.
[19] G. Pistoia (Ed.), Lithium Batteries: New Materials, Developments, and Perspectives, Industrial Chemistry Library, Elsevier, Amsterdam ; New York, 1994.
[20] M. Letellier, F. Chevallier, M. Morcrette, In situ 7Li nuclear magnetic resonance observation of the electrochemical intercalation of lithium in graphite; 1st cycle, Carbon 45 (5) (2007) 1025–1034, https://doi.org/10.1016/j.carbon.2006.12.018.
[21] M. Letellier, F. Chevallier, F. Béguin, E. Frackowiak, J.-N. Rouzaud, The first in situ 7Li NMR study of the reversible lithium insertion mechanism in disorganised carbons, J. Phys. Chem. Solid. 65 (2) (2004) 245–251, https://doi.org/10.1016/j.jpcs.2003.10.022.
[22] J.-M. Tarascon, A.S. Gozdz, C. Schmutz, F. Shokoohi, P.C. Warren, Performance of bellcore’s plastic rechargeable Li-ion batteries, Solid State Ionics 86–88 (1996) 49–54, https://doi.org/10.1016/0167-2738(96)00330-X.
[23] E. Salager, V. Sarou-Kanian, M. Sathiya, M. Tang, J.-B. Leriche, P. Melin, Z. Wang, H. Vezin, C. Bessada, M. Deschamps, J.-M. Tarascon, Solid-state NMR of the family of positive electrode materials Li2Ru1–ySnyO3 for lithium-ion batteries, Chem. Mater. 26 (24) (2014) 7009–7019, https://doi.org/10.1021/cm503280s.
[24] K. Shimoda, M. Murakami, D. Takamatsu, H. Arai, Y. Uchimoto, Z. Ogumi, In situ NMR observation of the lithium extraction/insertion from LiCoO2 cathode, Electrochim. Acta 108 (2013) 343–349, https://doi.org/10.1016/j.electacta.2013.06.120.
[25] L. Zhou, M. Leskes, A.J. Ilott, N.M. Trease, C.P. Grey, Paramagnetic electrodes and bulk magnetic susceptibility effects in the in situ NMR studies of batteries: application to Li1.08Mn1.92O4 spinels, J. Magn. Reson. 234 (2013) 44–57, https://doi.org/10.1016/j.jmr.2013.05.011.
[26] F. Poli, J.S. Kshetrimayum, L. Monconduit, M. Letellier, New cell design for in-situ NMR studies of lithium-ion batteries, Electrochem. Commun. 13 (12) (2011) 1293–1295, https://doi.org/10.1016/j.elecom.2011.07.019.
[27] A.I. Freytag, A.D. Pauric, S.A. Krachkovskiy, G.R. Goward, In situ magic-angle spinning 7Li NMR analysis of a full electrochemical lithium-ion battery using a jelly roll cell design, J. Am. Chem. Soc. 141 (35) (2019) 13758–13761, https://doi.org/10.1021/jacs.9b06885.
[28] X. Feng, M. Tang, S. O’Neill, Y.-Y. Hu, In situ synthesis and in operando NMR studies of a high-performance Ni5P4-nanosheet anode, J. Mater. Chem. A 6 (44) (2018) 22240–22247, https://doi.org/10.1039/C8TA05433A.
[29] E.G. Sorte, N.A. Banek, M.J. Wagner, T.M. Alam, Y. Tong, J. In situ stripline electrochemical NMR for batteries, Chemelectrochem 5 (17) (2018) 2336–2340, https://doi.org/10.1002/celc.201800434.
[30] O. Pecher, P.M. Bayley, H. Liu, Z. Liu, N.M. Trease, C.P. Grey, Automatic tuning matching cycler (ATMC) in situ NMR spectroscopy as a novel approach for real-time investigations of Li- and Na-ion batteries, J. Magn. Reson. 265 (2016) 200–209, https://doi.org/10.1016/j.jmr.2016.02.008.
[31] B.J. Walder, M.S. Conradi, J.J. Borchardt, L.C. Merrill, E.G. Sorte, E.J. Deichmann, T.M. Anderson, T.M. Alam, K.L. Harrison, NMR spectroscopy of coin cell batteries with metal casings, Sci. Adv. 7 (37) (2021), eabg8298, https://doi.org/10.1126/sciadv.abg8298.
[32] K. Märker, C. Xu, C.P. Grey, Operando NMR of nmc811/graphite lithium-ion batteries: structure, dynamics, and lithium metal deposition, J. Am. Chem. Soc. 142 (41) (2020) 17447–17456, https://doi.org/10.1021/jacs.0c06727.
[33] M. Gauthier, M.H. Nguyen, L. Blondeau, E. Foy, A. Wong, Operando NMR characterization of a metal-air battery using a double-compartment cell design, Solid State Nucl. Magn. Reson. 113 (2021), 101731, https://doi.org/10.1016/j.ssnmr.2021.101731.
[34] K. Ersching, C.E.M. Campos, J.C. de Lima, T.A. Grandi, Structural and thermal studies of mechanical alloyed InSb nanocrystals, Mater. Chem. Phys. 112 (3) (2008) 745–748, https://doi.org/10.1016/j.matchemphys.2008.08.054.
[35] M.A. Cambaz, B.P. Vinayan, O. Clemens, A.R. Munnangi, V.S.K. Chakravadhanula, C. Kübel, M. Fichtner, Vanadium oxyfluoride/few-layer graphene composite as a high-performance cathode material for lithium batteries, Inorg. Chem. 55 (8) (2016) 3789–3796, https://doi.org/10.1021/acs.inorgchem.5b02687.
[36] H.J. Chang, A.J. Ilott, N.M. Trease, M. Mohammadi, A. Jerschow, C.P. Grey, Correlating microstructural lithium metal growth with electrolyte salt depletion in lithium batteries using 7Li MRI, J. Am. Chem. Soc. 137 (48) (2015) 15209–15216, https://doi.org/10.1021/jacs.5b09385.
[37] P. Kukic, D. Farrell, L.P. McIntosh, B.G.-M. E, K.S. Jensen, Z. Toleikis, K. Teilum, J. E. Nielsen, Protein dielectric constants determined from NMR chemical shift perturbations, J. Am. Chem. Soc. 135 (45) (2013), 16968, https://doi.org/10.1021/ja406995j.
[38] Hao Wang, Alexander C. Forse, John M. Griffin, Nicole M. Trease, Lorie Trognko, Pierre-Louis Taberna, Patrice Simon, P. Clare, Grey, In situ NMR spectroscopy of supercapacitors: insight into the charge storage mechanism, J. Am. Chem. Soc. 135 (50) (2013) 18968–18980. https://pubs.acs.org/doi/10.1021/ja410287s, 2021-10-05.
[39] S.R. Sivakkumar, J.Y. Nerkar, A.G. Pandolfo, Rate capability of graphite materials as negative electrodes in lithium-ion capacitors, Electrochim. Acta 55 (9) (2010) 3330–3335, https://doi.org/10.1016/j.electacta.2010.01.059.
[40] N.M. Trease, L. Zhou, H.J. Chang, B.Y. Zhu, C.P. Grey, In situ NMR of lithium ion batteries: bulk susceptibility effects and practical considerations, Solid State Nucl. Magn. Reson. 42 (2012) 62–70, https://doi.org/10.1016/j.ssnmr.2012.01.004.
[41] R. Chen, S. Ren, M. Knapp, D. Wang, R. Witter, M. Fichtner, H. Hahn, Disordered lithium-rich oxyfluoride as a stable host for enhanced Li+ intercalation storage, Adv. Energy Mater. 5 (9) (2015), 1401814, https://doi.org/10.1002/aenm.201401814.